FULL PAPER

Dalton
www.rsc.org/dalton

Hybrid materials containing organometallic cations and 3-D anionic metal dicyanamide networks of type $[Cp^*_2M][M'(dca)_3]$

Patricia M. Van der Werff,[a] Eugenia Martínez-Ferrero,[b] Stuart R Batten,[b] Paul Jensen,[c] Catalina Ruiz-Pérez,[d] Manuel Almeida,[e] Joao C. Waerenborgh,[e] John D. Cashion,[f] Boujemaa Moubaraki,[a] José Ramón Galán-Mascarós,[b] José María Martínez-Agudo,[b] Eugenio Coronado*[b] and Keith S. Murray*[a]

[a] *School of Chemistry, Building 23, Monash University, 3800, Victoria, Australia. E-mail: keith.murray@sci.monash.edu.au; Fax: 61399054597; Tel: 61399054512*

[b] *Instituto de Ciencia Molecular, Universidad de Valencia, Dr. Moliner, 50, 46100, Burjassot, Spain*

[c] *Department of Chemistry, Trinity College, Dublin 2, Ireland*

[d] *Laboratorio de Rayos X y Materiales Moleculares, Departamento de Física Fundamental II, Universidad de La Laguna, Avda. Francisco Sanches sw/n, E-38204, La Laguna, Tenerife, Spain*

[e] *Dept. Química, ITN/CFMC-UL, P-2686-953, Sacavém, Portugal*

[f] *School of Physics and Materials Engineering, Building 27, Monash University, 3800, Victoria, Australia*

Received 1st October 2004, Accepted 19th November 2004
First published as an Advance Article on the web 3rd December 2004

A new series of hybrid materials of type $[Cp^*_2M][M'(dca)_3]$ has been prepared by cation templation and structurally characterised (M = Fe(III), Co(III); M′ = Mn(II), Fe(II), Co(II), Ni(II), Cd(II); $dca^- = N(CN)_2^-$). The crystallographic analysis of $[Cp^*_2Fe][Cd(dca)_3]$ showed that the $[Cd(dca)_3]^-$ anionic framework is of a symmetrical 3-D α-polonium type, containing octahedral Cd nodes and $\mu_{1,5}$-dca bridging ligands. The $[Cp^*_2Fe]^+$ cations occupy the cube-like cavities within the framework. The cationic and anionic-framework sublattices remain magnetically independent and display susceptibilities, over the range 300 to 2 K, of a Curie–Weiss nature obtained by adding a $S = 1/2$ ($Cp^*_2Fe^+$) or a $S = 0$ ($Cp^*_2Co^+$) contribution to those of the weakly antiferromagnetically coupled frameworks of M′. These hybrid species do not show any intrinsic long-range magnetic order. The present $[Cp^*_2Fe][M'(dca)_3]$ series display the characteristic, unusually shaped $[Cp^*_2Fe]^+$ Mössbauer line, in the range 295–5 K, assigned (below 101 K) as the sum of a narrow and a broad line. Relaxation effects were evident. The $[Fe(dca)_3]^-$ compound showed superimposed low-spin Fe(III) and high-spin Fe(II) lines, the latter giving relaxation broadening effects.

Introduction

As part of an extensive study of d-block metal dicyanamide molecular magnetic materials[1,2] we are developing hybrid species containing paramagnetic organometallic or organic cations combined with polymeric anionic dicyanamidometallate networks. We have recently reported such anionic framework structures in which the cation is a non-magnetic quaternary organic moiety,[3] such as Ph_4As^+, or a paramagnetic metal 2,2′-bipyridine complex,[4] such as $Ni(bipy)_3^{2+}$. The cations act as templates in the formation of the inorganic network. Studies of the magnetic interactions within the anionic network and between the paramagnetic cationic and anionic sublattices are of particular interest.

In the present paper, we report the synthesis, crystal structure, magnetic and Mössbauer spectral properties of a series of isostructural 3-D $[M'(N(CN)_2)_3)]^-$ ($[M'(dca)_3]^-$) framework compounds in which decamethylferrocenium (d^5 low-spin) or decamethylcobaltocenium (d^6 low-spin) organometallic π-sandwich complexes are held in the cavities of the framework. There were a number of reasons for investigating such materials. They represent the first examples of hybrid organometallic cation salts of anionic metal dicyanamido frameworks. It was anticipated that the size and shape of these cations would influence the topology of the $[M'(dca)_3]^-$ network differently to the above-mentioned cations.[3,4] Second, it was important to discover if the spins on the decamethylferrocenium cations would interact with the weakly coupled spins on the $[M'(dca)_3]^-$ frameworks, even though they are not covalently bonded to the latter. It is known that such 'through space' (spin polarisation) interactions occur in the prototypical chain-like ferromagnetic radical salt $[Cp^*_2Fe][TCNE]$.[5] The decamethylferrocenium cations might provide a more effective spin interaction than was the case[4] with $Ni(bipy)_3^{2+}$. Third, we wished to make comparisons with related hybrid materials containing decamethylmetallocenium cations and anionic oxalatometallate frameworks, the latter being generally heterometallic and displaying long-range magnetic order and thus different in magnetic character to the present homometallic $[M'(dca)_3]^-$ species. In this context, some of the present authors[6–8] have made extensive studies on $Cp^*_2Fe^+$ (and Co) derivatives of the 2-D layered oxalato bridged magnets, $[M(II)M'(III)(C_2O_4)_3]^-$ and these compounds have generally exhibited independent cation and anion magnetic sublattices. The $Cp^*_2Fe^+$ cation has also been incorporated into other related species containing paramagnetic Ni(III) thiolato anions[9] or polyoxometallate cluster anions.[10,11]

Experimental

Synthesis

The synthesis of K(dca) was carried out as described previously.[3] The synthesis of $[Cp^*_2Fe]BF_4$ followed the literature method.[12] $[Cp^*_2Co]PF_6$ and Cp^*_2Fe were purchased from Sigma-Aldrich Pty. Ltd. Na(dca) was kindly donated by Degussa AG, Trostberg, Germany.

$[Cp^*_2Fe][Mn(dca)_3]$. $Mn(NO_3)_2{\cdot}4H_2O$ (0.050 g, 0.199 mmol) in ethanol (5 mL) was added to a solution of K(dca) (0.064 g,

DOI: 10.1039/b415275a

0.609 mmol) in ethanol (10 mL). The resulting KNO_3 was filtered off and the filtrate added to a solution of $[Cp^*_2Fe]BF_4$ (0.084 mg, 0.204 mmol) in ethanol (20 mL). After 60 min, emerald green block-shaped crystals had started forming on the sides of the vial. Some were multiple crystals. After several days crystals were collected (yield: 0.072 g, 63%), washed with water, then ethanol. Calc. for $C_{26}H_{30}N_9FeMn$: C, 53.90; H, 5.22; N, 21.76. Found: C, 53.30; H, 5.34; N, 21.50%. IR (KBr, cm^{-1}): 3066vw, 2977w, 2921w, 2299s, 2239m, 2175vs, 1475m, 1424w, 1376s, 107444w, 1022m, 910w, 642w, 505m, 444w.

Better quality crystals were grown by slow diffusion in a 10 mL capacity H-tube. $[Cp^*_2Fe]BF_4$ (0.021 g, 0.048 mmol) was dissolved in 3 mL of ethanol and pipetted into one side of the H-tube. $Mn(NO_3)_2{\cdot}4H_2O$ (0.013 g, 0.052 mmol) and K(dca) (0.016 g, 0.152 mmol) were dissolved in 3 mL of ethanol and filtered into the other side. The H-tube was then carefully filled with ethanol. After 5 days good quality emerald green crystals had grown. Unit cell (123 K): cubic I, $a = 17.601(2)$ Å.

$[Cp^*_2Fe][Fe(dca)_3]$. $Fe(ClO_4)_2$ (0.2 g, 0.77 mmol) and Na(dca) (0.21 g, 2.3 mmol) were dissolved in a 1 : 1 EtOH–H_2O mixture (20 mL). This solution was added, dropwise, to an ethanolic solution (20 mL) of $[Cp^*_2Fe]BF_4$ (0.16 g, 0.39 mmol) to give a green solution. Several crops of crystals were collected on successive days. Yield (after 4 days): 0.16 g, 68%.

Calc. for $C_{26}H_{30}N_9Fe_2$: C, 53.82; H, 5.21; N, 21.72. Found: C, 52.98; H, 5.67; N, 21.66%. IR (KBr, cm^{-1}): 3065vw, 2975w, 2922w, 2300s, 2240m, 2181vs, 1475w, 1424vw, 1378s, 1075vw, 1023w, 906vw, 634w, 497w.

$[Cp^*_2Fe][Co(dca)_3]$. This was prepared in the same way as the Mn complex. Green block-shaped crystals were collected (0.139 g, 39%). Calc. for $C_{26}H_{30}N_9FeCo$: C, 53.52; H, 5.18; N, 21.61. Found: C, 53.32; H, 5.17; N, 21.51%. IR (KBr, cm^{-1}): 3065vw, 2978vw, 2923vw, 2304s, 2245m, 2186vs, 1477w, 1423vw, 1385s, 1076vw, 1024w, 903vw, 631w, 496w, 446vw. Unit cell (123 K): cubic I, $a = 17.419(2)$ Å.

$[Cp^*_2Fe][Ni(dca)_3]$. This was prepared in the same way as the Mn complex. The product (0.149 g, 42%) consisted of green microcrystalline material (0.093 g) from the bottom of the vials, and green block-shaped crystals (0.056 g) from the sides. The latter sample was used for all analysis. Calc. for $C_{26}H_{30}N_9FeNi$: C, 53.55; H, 5.19; N, 21.62. Found: C, 52.90; H, 5.13; N, 21.24%. IR (KBr, cm^{-1}): 2925vw, 2309m, 2250w, 2192vs, 1477w, 1387m, 12078vw, 1024w, 901vw, 671vw, 626vw, 492w.

Good quality crystals were grown by slow diffusion in a 10 mL capacity H-tube, in a similar manner to that described above. Unit cell (123 K): cubic I, $a = 17.314(4)$ Å.

$[Cp^*_2Fe][Cd(dca)_3]$. This was prepared in the same way as the Mn complex. The product (0.161 g, 62%) consisted of green cubic crystals from the bottom (0.119 g) and sides (0.042 g) of the vial. The latter was used for all analysis, including X-ray diffraction study, reported herein. Calc. for $C_{26}H_{30}N_9FeCd$: C, 49.03; H, 4.75; N, 19.80. Found: C, 48.80; H, 4.61; N, 19.70%. IR (KBr, cm^{-1}): 3068vw, 2978vw, 2918vw, 2295s, 2240m, 2177vs, 1476w, 1424vw, 1368m, 1074vw, 1023w, 917vw, 650w, 507m, 445w.

$[Cp^*_2Co][Mn(dca)_3]$. K(dca) (0.158 mg, 1.503 mmol) was dissolved in ethanol (25 mL). $Mn(NO_3)_2{\cdot}4H_2O$ (0.126 g, 0.503 mmol) was added, and the KNO_3 filtered off. $[Cp^*_2Co]PF_6$ (0.237 g, 0.500 mmol) in DMF (5 mL) was then added. After 24 h, yellow block-shaped crystals (0.093 g, 32%) were collected from the sides and bottom of the vial, and washed with ethanol. Calc. for $C_{26}H_{30}N_9CoMn$: C, 53.6; H, 5.2; N, 21.7. Found: C, 54.1; H, 5.1; N, 21.8%. IR (KBr, cm^{-1}): 3068vw, 2983vw, 2921vw, 2298s, 2239m, 2177vs, 1478w, 1427vw, 1377m, 1078vw, 1025w, 913vw, 644vw, 506w. Unit cell (123 K): cubic I, $a = 17.573$ (2) Å.

$[Cp^*_2Co][Co(dca)_3]$. This was prepared as for $[Cp^*_2Co][Mn(dca)_3]$ except that $[Cp^*_2Co]PF_6$ was dissolved in CH_3CN. Small block-shaped mustard yellow micro-crystals (0.167 g, 57%) were collected and washed with ethanol. Calc. for $C_{26}H_{30}N_9Co_2$: C, 53.24; H, 5.16; N, 21.50. Found: C, 52.71; H, 5.10; N, 21.92%. IR (KBr, cm^{-1}): 3067vw, 2981vw, 2923vw, 2303s, 2246m, 2187s, 1478m, 1448vw, 1426vw, 1384s, 1078w, 1025m, 905w, 631w, 497m, 442w.

High quality crystals were grown by slow diffusion in a 10 mL capacity H-tube. $[Cp^*_2Co]PF_6$ (0.027 g, 0.057 mmol) was added to one side of the H-tube and $Co(NO_3)_2{\cdot}6H_2O$ (0.030 g 0.103 mmol) and K(dca) (0.031 mg 0.295 mmol) were added to the other side. CH_3CN (1 mL) was added to the side containing the metal and K(dca). The H-tube was then carefully filled with ethanol. Crystals grew after several days. Unit cell (123 K): cubic I, $a = 17.385(2)$ Å.

$[Cp^*_2Co][Ni(dca)_3]$. This was prepared as for $[Cp^*_2Co][Co(dca)_3]$. A lime-green microcrystalline powder (0.148 g, 50%) was collected. Calc. for $C_{26}H_{30}N_9CoNi$: C, 53.21; H, 5.16; N, 21.51. Found: C, 52.71; H, 5.06; N, 21.33%. IR (KBr, cm^{-1}): 2967vw, 2924vw, 2307s, 2251m, 2194vs, 1478w, 1387s, 1079vw, 1025w, 900vw, 628w, 491w, 443vw.

Crystals were grown in the way used for $[Cp^*_2Co][Co(dca)_3]$. Unit cell (123 K): cubic I, $a = 17.287(2)$ Å.

Crystallography

An X-ray structural analysis for $[Cp^*_2Fe][Cd(dca)_3]$ was performed at Monash University with a Nonius KappaCCD diffractometer using graphite monochromated Mo-Kα radiation ($\lambda = 0.71073$ Å). Data were collected, processed and corrected for Lorentzian and polarization effects using Nonius software.[13] A numerical absorption correction was applied using the XPREP program.[14] The structure was solved using direct methods and refined on F^2 using the SHELXL-97 program.[15]

Crystal data for $[Cp^*_2Fe][Cd(dca)_3]$: $C_{26}H_{30}CdFeN_9$, $M = 636.84$, cubic, space group $Im\bar{3}$, $a = 17.712(2)$ Å, $V = 5556.5(11)$ Å^3, $Z = 8$, $T = 123$ K, $F(000) = 2584$, $D_c = 1.523$ g cm^{-1}, μ(Mo-Kα) = 1.319 mm^{-1}, green cube (0.10 × 0.10 × 0.10 mm), 31270 reflections, 905 unique ($R_{int} = 0.0723$), two component twin refinement, 59 parameters, BASF (twin component) = 0.55(2), $R_1 = 0.0808$ (596 reflections, $I > 2\sigma(I)$), $wR_2 = 0.1903$ (all data), $S = 1.169$.

The overall structure has a cubic I cell, however the high symmetry relationship of the heavy atoms within this cell means that the data corresponding to a possible F centred lattice (*i.e.* 3/4 of the data) are very weak with respect to the other data. If the light atoms are ignored, the lattice of metal ions is both F and I centred on the original cell. This 'sub-lattice' reduces to a primitive cubic cell with one metal type at the corners, the other at the body centre, and cell lengths half those of the original cubic I cell. This highlights the fact that with the correct cubic I cell, only the light atoms contribute to a large class of data (*i.e.* those corresponding to the F lattice exception). All the light atoms, except the coordinated nitrogen atoms, were refined with disorder. The carbon and amide nitrogen atoms of the dca ligand are disordered over two positions. One half of the dca ligand is related to the other since both amide nitrogen positions reside on a mirror plane. However, no symmetry relates the two disordered dca positions, with half of each specified in the asymmetric unit.

Since $Im\bar{3}$ belongs to the lower symmetry cubic Laue group, $m\bar{3}$, merohedral twinning may occur so that the structural solution looks like the higher symmetry $m\bar{3}m$ Laue group. This was the case with the present refinement. The initial solution containing the metal atoms and coordinating nitrogen atom refined poorly with residual electron density indicating four disordered positions for the dca ligand. Introduction of a twin refinement improved the model giving just two disordered positions for the dca ligand. The R_{int} for $m\bar{3}m$ was slightly higher than for $m\bar{3}$ (0.077 *cf.* 0.072) which is typical when this type of twinning is present with approximately equal domains. From close analysis of the structure it is clear that the network does not

possess two-fold symmetry about the face diagonals (a symmetry element of the $m\bar{3}m$ Laue group). This is the operator that relates the two twin domain orientations in the present refinement. The twin law is {010 100 00$\bar{1}$} with the twin component refining to 0.55(2) indicating approximately equal amounts of the two domains.

The Cp* ligands are disordered as dictated by the symmetry of $Im\bar{3}$ and were refined as rigid groups at the required reduced occupancy and with the necessary restraints to keep the Fe–C distances comparable to known $[Cp^*_2Fe]^+$ structures. One Cp* ligand position is specified for each cation with inversion symmetry generating the other half of the π-sandwich complex. The Fe1 cations which reside on intersecting two-fold and three-fold axes, are disordered over twelve positions. The Fe2 cations, however, reside only on intersecting two-fold axes and are disordered over four positions.

The twin refinement combined with the disorder required a full arsenal of constraints and restraints to keep reasonable bond distances, angles, *etc.* for the ligands. When the heavy atoms correspond to higher symmetry, as is the case in the present systems, it can be very difficult to distinguish between twinning and disorder of the light atoms.[16] Of the compounds reported here, the $[Cd(dca)_3]^-$ network provides the largest host for the $[Cp^*_2Fe]^+$ cations and therefore is perhaps most likely to contain disorder. This is consistent with the thermal diffuse scattering evident in the CCD diffraction images. It is possible, however, that the crystals contain further twinning with less disorder of the light atoms. This is perhaps more likely to be the case for the smaller host networks (*e.g.* where M′ = Ni). Analysis of such problems are of specialist crystallographic interest. In the present study, unit cell determinations and powder X-ray diffraction were used to confirm the homogeneity of the $[Cp^*_2M][M'(dca)_3]$ series.

CCDC reference number 242153.

See http://www.rsc.org/suppdata/dt/b4/b415275a/ for crystallographic data in CIF or other electronic format.

Mössbauer and magnetic measurements

Mössbauer effect measurements were made at Monash University and at ITN, Sacavém, Portugal. ^{57}Fe Mössbauer measurements were recorded in transmission mode using a conventional constant acceleration spectrometer and a 25 mCi ^{57}Co source in the Rh matrix. The velocity scale was calibrated using an α-Fe foil at room temperature. Isomer shift values are given relative to this standard. Spectra were collected with the absorbers between 296 and 5 K. Low-temperature measurements were obtained using a flow cryostat (temperature stability ± 0.5 K). The spectra were fitted to Lorentzian lines using a nonlinear least-squares fitting method.

Magnetic susceptibility measurements were made at Monash University using a Quantum Design MPMS 5 Squid magnetometer for DC studies, in a field of 1 T, and at the University of Valencia in a field of 0.1 T. The results were in excellent agreement. A Quantum Design PPMS instrument was used at Monash for ac susceptibilities with a frequency of 10 Hz and a field of 0.5 Oe. In the cases of compounds having orbitally degenerate M′(II) ions within the anionic network, the powders were dispersed in Vaseline mulls in order to prevent crystallite torquing and consequent anomalous data.

Results and discussion

Synthesis and characterization

The $[Cp^*_2M][M'(dca)_3]$ compounds were made by forming ethanolic solutions of stoichiometry M′ : dca = 3 : 1, using the M′(II) nitrate or perchlorate (Fe) salt added to K(dca) (or Na(dca) for the $[Cp^*_2Fe][Fe(dca)_3]$ complex). After filtration of KNO_3 ($NaClO_4$ remained in ethanol solution), these solutions were added to an ethanolic solution of the templating $[Cp^*_2M]^+$ salt. Well formed crystals of product generally formed upon standing or by careful slow diffusion methods in H-tubes.

Crystal structures

Crystal structure analyses have been very challenging and have revealed the structure of the anionic $[M'(dca)_3]^-$ framework to be of the 3-D α-Po type, as was found recently in some quaternary ammonium salts.[17] Unlike the previously reported cubic-like networks,[17] which are clearly distorted to primitive orthorhombic symmetry, the present networks display *I*-centred cubic (or at least pseudo-cubic) symmetry. Crystals of $[Cp^*_2Fe][Mn(dca)_3]$ give weak 'satellite' reflections (in addition to those indexing to the 'parent' cubic *I* cell) indicative of a modulated or superstructure.[18] This phenomenon was not observed for any of the other compounds, however it demonstrates that subtle variations in the packing of the organic moieties may give different crystallographic symmetry for different combinations of M and M′, despite the high metric symmetry of the unit cell. In the present study, single crystal data for all $[Cp^*_2M][M'(dca)_3]$ compounds indexed to cubic *I*-centred unit cells indicating that they are essentially isostructural (see Experimental section).

The structural refinement presented here is that of $[Cp^*_2Fe][Cd(dca)_3]$ with cubic $Im\bar{3}$ symmetry. This structure was chosen partly because the difference in scattering power between the Fe and Cd atoms allowed assignment of these respective metals with confidence, particularly in light of the high disorder of the organic moieties. The X-ray powder diffractogram calculated from the crystal structure of $[Cp^*_2Fe][Cd(dca)_3]$ compared well with that measured for the bulk sample and also with the powder data measured on other bulk samples in the series. The structure of the $[Cd(dca)_3]^-$ network and the positions of the Fe atoms within it are shown in Fig. 1. All metal atoms sit on special positions. There is one unique Cd position and two unique Fe positions. The Cd atoms reside at 1/4, 1/4, 1/4 and the seven other equivalent positions in each unit cell. The Fe1 atoms reside at the corners and centre of each unit cell, while the Fe2 atoms reside at the centre of each cell edge and face. Thus, there are three times as many Fe2 atoms (6 per cell) as there are Fe1 atoms (2 per cell) in the structure. Each Cd atom resides on an inversion centre, three perpendicular two-fold screw axes (along the principal cell directions), and a single three-fold axis (along the appropriate body diagonal). As a result, a beautiful, highly symmetric 3D net, with α-Po topology, results from the connection of these Cd atoms by the bridging $\mu_{1,5}$-dca anions The dca anions are disordered over two positions, as shown in Fig. 1. This side-by-side disorder is similar to that observed in a number of other metal–dca structures.[19–21] The $Cp^*_2Fe^+$ cations lie in the cubic cavities of the network. Due to the high symmetry, the Cp* rings are highly disordered, and thus only the metal positions are shown in Fig. 1.

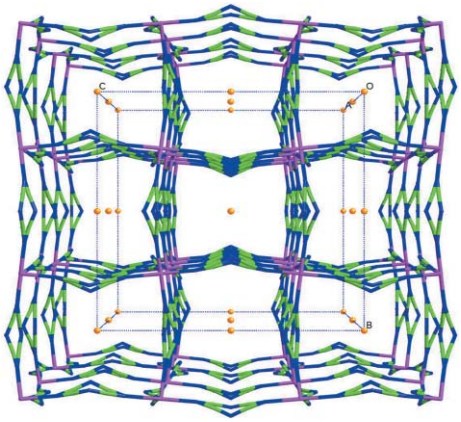

Fig. 1 Structure of the $[Cp^*_2Fe][Cd(dca)_3]$ network. Only the Fe atoms of the Cp^*_2Fe groups are shown (see text).

The Cd–N distance refined to 2.30(1) Å with coordination bond angles very close (within *ca.* 1°) to perfect octahedral symmetry. The closest M–M distances are equal to $a/2$ (8.856(2) Å) for like metals and $\sqrt{3}a/4$ (7.670(2) Å) for Cd–Fe (*i.e.* 1/4 of the body diagonal).

Mössbauer effect

Spectra of the Mn(II) sample are shown in Fig. 2, together with the fitted components. At 295 K, a single, slightly asymmetric line is observed. This is interpreted as an unresolved quadrupole doublet corresponding to the low-spin Fe(III) from the decamethylferrocenium cation. The parameters (labelled as (1) in Table 1) agree with literature data on decamethylferrocenium salts.[7]

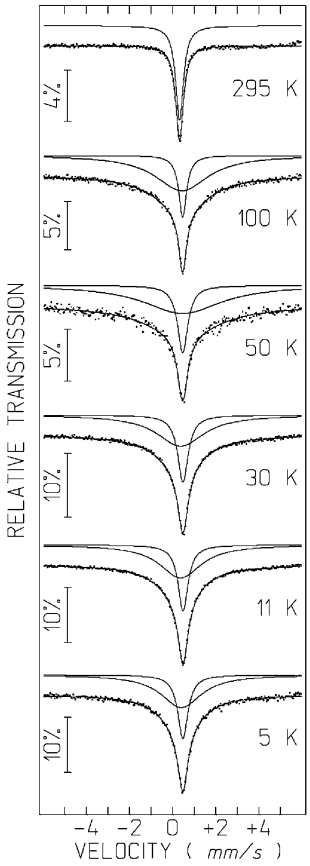

Fig. 2 Mössbauer spectra in the range 295–5 K for $[Cp^*_2Fe][Mn(dca)_3]$.

At lower temperatures, the spectrum broadens and can be fitted with the sum of a narrow Lorentzian line and an extremely broad Lorentzian line (labelled as (2) in Table 1). The broadening is caused by slow paramagnetic relaxation as already observed in other decamethylferrocenium compounds.[7]

Table 1 Mössbauer spectral parameters (isomer shift, δ, and line width, Γ) for $[Cp^*_2Fe][Mn(dca)_3]$

T/K	$[Cp^*_2Fe]$ line	δ/mm s^{-1}	Γ/mm s^{-1}
295	(1)	0.43(1)	0.43(1)
101	(1)	0.57(1)	0.44(2)
	(2)	0.54(2)	3.0(1)
50	(1)	0.58(1)	0.58(3)
	(2)	0.58(2)	4.4(5)
30	(1)	0.59(1)	0.59(5)
	(2)	0.48(2)	2.7(1)
11	(1)	0.59(1)	0.56(1)
	(2)	0.48(2)	2.3(1)
5	(1)	0.59(1)	0.57(1)
	(2)	0.51(2)	2.3(1)

Table 2 Mössbauer parameters (isomer shift, δ, and line width, Γ) at 82 K of four samples

Sample	Component	δ/mm s^{-1}	Γ/mm s^{-1}
Ni	1	0.53(1)	0.66
	2	0.56(3)	4.40
Mn	1	0.53(1)	0.62
	2	0.55(3)	4.72
Co	1	0.54(1)	0.62
	2	0.55(1)	4.32
Cd	1	0.57(1)	0.62
	2	0.47(3)	4.86

The spectra at 82 K of four members of the present series, $[Cp^*_2Fe][M(dca)_3]$, where M = Mn, Co, Ni and Cd were almost identical and the fitted parameters are given in Table 2. The isomer shifts of the two fitted components for the spectrum of the diamagnetic cadmium compound moved in opposite directions compared to the spectra for the other samples. The area ratio of the narrow to broad components appeared to be constant within ±2% at 25 : 75% in spectra taken at moderate velocities of ~±6 mm s^{-1}, consistent with assigning the two components to the two different iron sites. However, a spectrum taken at ±13 mm s^{-1} showed evidence of splitting out to nearly 10 mm s^{-1}, and relative areas of 16 : 84%, making the assignment uncertain and providing evidence of a very large hyperfine field.

The Mössbauer spectrum of the Fe(II)-containing sample (Fig. 3) clearly has two different components at room temperature. The left-hand, slightly asymmetric, dip corresponds to the low-spin Fe(III) of the $[Cp^*_2Fe]$ cation as before. The right-hand doublet with the large quadrupole splitting corresponds to the high-spin $Fe(dca)_3^-$ ion (parameters in Table 3). At low temperatures, the low-spin Fe(III) component broadens due to the reduction in the paramagnetic relaxation rate, but this is not as pronounced as in the other samples because of the enhanced spin-spin relaxation provided by the strongly paramagnetic Fe(II). The quadrupole splitting of the Fe(II) component shows a marked increase as the temperature is reduced, due to the depopulation of excited crystal field levels.

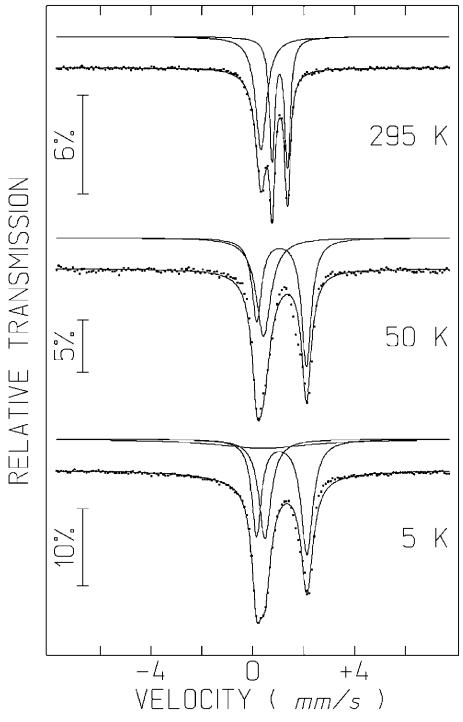

Fig. 3 Mössbauer spectra of $[Cp^*_2Fe][Fe(dca)_3]$ at the temperatures shown.

Table 3 Mössbauer parameters (isomer shift, δ, line width, Γ, and quadrupole splitting Δ) estimated for the Fe(II) compound

	T/K	δ/mm s^{-1}	Γ/mm s^{-1}	Δ/mm s^{-1}
[Cp*$_2$Fe] (1)	295	0.43(1)	0.49(1)	—
Fe(II)–dca	295	1.17(1)	0.23(1)	0.60(1)
[Cp*$_2$Fe] (1)	50	0.54(1)	0.69(1)	—
Fe(II)–dca	50	1.24(1)	0.27(1)	1.96(1)
[Cp*$_2$Fe] (1)	5	0.59	0.56(1)	—
[Cp*$_2$Fe] (2)	5	0.53(1)	3.9(3)	—
Fe(II)–dca	5	1.25(1)	0.38(1)	1.99(1)

Magnetism

In the [Cp*$_2$Co]$^+$ series, the temperature dependence of the effective magnetic moment, μ_{eff}, is similar to those we reported for the [Ph$_4$As][M′(dca)$_3$] compounds[3] since the t_{2g}^6 cobaltocenium cation is essentially diamagnetic. For example, the M′ = Mn complex shows Curie–Weiss $S = 5/2$ susceptibility behaviour with $C = 4.35$ cm^3 mol^{-1} K and $\theta = -3.5$ K and has corresponding temperature-independent μ_{eff} values of 5.86 μ_B ($\chi T = 4.29$ cm^3 mol^{-1} K) between 300 K and ~50 K. The μ_{eff} values then decrease rapidly to reach 4.5 μ_B at 4.2 K because of very weak antiferromagnetic coupling between adjacent Mn (d^5) ions combined with zero-field splitting of the single-ion $^6A_{1g}$ states (Fig. 4). A good fit of the μ_{eff}/T data was obtained when using a 2-D Heisenberg model, [22] with $g = 1.99$ and $J = -0.096$ cm^{-1}. The same result was obtained using a 3-D model.[3] The J value, while small, is similar in size to those obtained for the 2-D Ph$_4$P$^+$ and Ph$_4$As$^+$ salts[3] but a little less than the value noted for the (different) 3-D MePh$_3$P$^+$ salt.[3] There was no evidence for long-range magnetic ordering in [Cp*$_2$Co][Mn(dca)$_3$] when magnetizations were measured in very small fields of magnitude 20 Oe or in zero-field cooled mode. The magnetic moments were independent of applied field at all temperatures. The [Cp*$_2$Co][Co(dca)$_3$] complex shows typical $^4T_{1g}$ behaviour between 300 and 20 K with $C = 3.45$ cm^3 mol^{-1} K and $\theta = -30.1$ K. The large, negative value of θ results from a combination of spin–orbit coupling/low-symmetry ligand field splitting as well as weak exchange coupling. An unusual dependence of moment with field occurs at very low temperatures, as noted for the Ph$_4$As$^+$ system,[3] and is due, probably, to weak short range ferromagnetic coupling. The [Cp*$_2$Co][Ni(dca)$_3$] compound is described below.

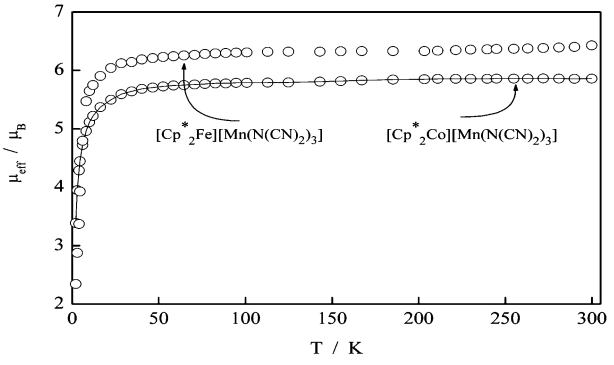

Fig. 4 Plots of magnetic moment, per mol, in a field of 1 T for the Cp*$_2$Fe$^+$ and Cp*$_2$Co$^+$ salts of [Mn(dca)$_3$]$^-$. Note that $\chi T = (\mu_{eff})^2/7.997$. The solid line is the calculated plot using the parameters given in the text.

In the [Cp*$_2$Fe][M′(dca)$_3$] series, the M′ = Cd compound behaves in the Curie–Weiss way observed for [Cp*$_2$Fe](BF$_4$)[23] and expected for a distorted $^2T_{2g}$ Fe(III) octahedral complex, with $C = 0.74$ cm^3 mol^{-1} K and $\theta = -1.9$ K. The μ_{eff} values gradually decrease from 2.40 μ_B, at 300 K to 2.10 μ_B at 2 K. The M′ = Co and Mn compounds display the same type of behaviour observed for the Cp*$_2$Co$^+$ salts but with a superimposed Curie–Weiss contribution from the $S = 1/2$ [Cp*$_2$Fe]$^+$ centre. Thus, μ_{eff} for the Mn compound varies from 6.43 μ_B at 300 K, to 6.20 μ_B at 50 K, then decreases rapidly to 3.40 μ_B at 4.2 K due to weak coupling and zero field splitting effects. Calculation of the moment at 300 K expected for spin-only d^5 plus the [Cp*$_2$Fe][Cd(dca)$_3$] contribution is 6.37 μ_B, which compares well to the observed value. The Curie–Weiss constants are $C = 5.15$ cm^3 mol^{-1} K and $\theta = -3.5$ K. Low temperature magnetisation studies showed no evidence in this, or in the [Cp*$_2$Co][Mn(dca)$_3$] analogue, for long range magnetic order. The Curie–Weiss constants for [Cp*$_2$Fe][Co(dca)$_3$] are $C = 4.16$ cm^3 mol^{-1} K and $\theta = -20.6$ K, the high θ value arising from the orbital contribution to the moment on the Co(II) centres.

The two [Ni(dca)$_3$]$^-$ networks behave like the other [M′(dca)$_3$]$^-$ systems. Thus, in a field of 1 T both compounds show Curie–Weiss susceptibility behaviour with $C = 1.14$ (Cp*$_2$Co$^+$) and 1.78 (Cp*$_2$Fe$^+$) cm^3 mol^{-1} K with corresponding θ values of −0.19 and −1.25 K. A very small, gradual decrease in moment occurs between 300 to ~ 20 K (3.12 μ_B to 3.06 μ_B for the Cp*$_2$Co complex and 3.77 μ_B to 3.69 μ_B for the Cp*$_2$Fe complex (Fig. 5). In some, but not all of the repeat preparations, a small increase occurs below 20 K, to reach a maximum (3.09 μ_B for Cp*$_2$Co and 3.75 μ_B for Cp*$_2$Fe) before a more rapid decrease. Apart from the maximum at ~20 K, the behaviour in both compounds is due to weak antiferromagnetic coupling and zero field splitting within the [Ni(dca)$_3$]$^-$ networks. The 20 K behaviour is due to traces of a ferromagnetic impurity in these highly crystalline materials, most likely α-[Ni(dca)$_2$], as judged by use of low applied-dc fields (Fig. 5) and other ac magnetisation, hysteresis and ac susceptibility probes. The X-ray powder diffractograms did not display any peaks due to α-[Ni(dca)$_2$]. This is not surprising since trace quantities of α-[Ni(dca)$_2$] would be well below the detection limit of powder XRD. A similar situation was encountered in [Ph$_4$As][Ni(dca)$_3$].[3]

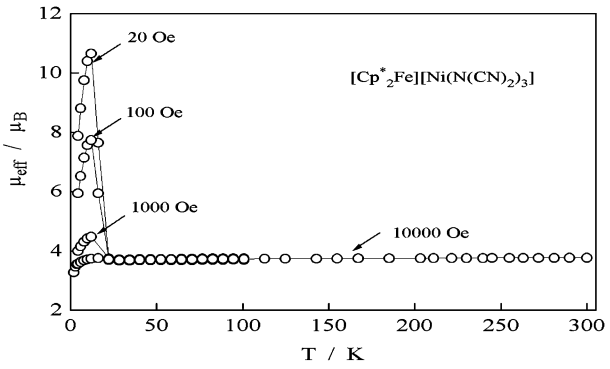

Fig. 5 Plots of magnetic moment, per mol, for [Cp*$_2$Fe][Ni(dca)$_3$] (Monash sample) in the applied fields shown. The solid lines just join the points.

Conclusions

In summary, the magnetic and Mössbauer data show that there is little, if any, electronic interaction between the paramagnetic cationic and the weakly coupled anionic sub-lattices. The weak coupling in the M′(dca)$_3^-$ lattice is due to the $\mu_{1,5}$-dca bridging mode which provides a poor superexchange pathway between the M′ ions and, consequently, to no long-range ordering occurring, even in 3-D networks.[1,2] Lack of cation–anion interaction is also the case in the decamethylferrocenium–polyoxometallate clusters,[10,11] decamethylferrocenium–hexahalorhenate(IV) salts[22] and the decamethylferrocenium–tris(oxalato) metallate 2-D materials, although the latter show strong magnetic order within their mixed-metal anionic networks.[6–8] Presumably the absence of magnetic interactions between cations and anionic networks in these systems is due to a combination of (i) lack of suitable interconnecting exchange pathways, (ii) symmetry

mismatches, (iii) domination of the exchange coupling within the anionic network (or within a polyoxometallate cluster) over the decamethylferrocenium $S = 1/2$ spins. In contrast, the donor–acceptor 1-D chain systems of type $[Cp^*_2Fe][TCNE]$ show strong magnetic interactions between the (radical) cation and anion spins,[5] but these have quite different topological and bonding ('through-space') modes to those of the above-mentioned derivatives.

The effects of cation variations upon magnetism can, however, be quite intriguing, even for diamagnetic cations of type $(R_xNH_{4-x})^+$. Thus, in contrast to the decamethylferrocenium salts of the bimetallic 2-D oxalate nets,[6–8] variations in the quaternary ammonium cation have been shown to influence the type of order and the T_c values originating within the metal–oxalate sublattice.[24,25] Similar effects have recently been noted in $(R_xNH_{4-x})^+$ salts of 3-D nets of $S = 5/2$ Fe(III) centres[26] contained within the mixed-ligand dianion $[Fe(C_2O_4)_2(Cl)_2(\mu\text{-}O)]^{2-}$. Canted spin antiferromagnetic order was observed, with T_c values as high as 56 K. The reason for long-range order occurring in these homometallic Fe(III) species, but not in the present $M'(dca)_3^-$ networks, is primarily because of the strong antiferromagnetic coupling provided by μ-oxalate and μ-oxo pathways compared to $\mu_{1,5}$-dca pathways. To achieve such behaviour in the dicyanamide anionic networks, whether combined with dia- or para-magnetic cations, we need to obtain $\mu_{1,3}$-dca bridging[1,2] probably combined with other stronger-coupling bridging groups such as cyanide or oxalate. Work is progressing in these directions.

Acknowledgements

The support of Australian Research Council (ARC) Discovery grants (to K. S. M., J. D. C., S. R. B.) and an Australian Research Fellowship (to S. R. B.) is gratefully acknowledged. In Valencia the work was supported by the European Union (COST Action on Inorganic Molecular Conductors) and by the Spanish Ministerio de Ciencia y Tecnología (MCyT) (Projects no. MAT2001-3507). E. M. F. thanks the McyT for a predoctoral fellowship. The authors wish to thank G. B. Jameson (Massey University, New Zealand) and S. Parsons (University of Edinburgh, UK) for useful crystallographic discussions.

References

1 S. R. Batten, P. Jensen, B. Moubaraki, K. S. Murray and R. Robson, *Chem. Commun.*, 1998, 439.
2 S. R. Batten and K. S. Murray, *Coord. Chem. Rev.*, 2003, **246**, 103. Full references to other workers in the metal dicyanamide field are given in this review.
3 (*a*) P. M. Van der Werff, S. R. Batten, P. Jensen, B. Moubaraki, K. S. Murray and E. H.-K. Tan, *Polyhedron*, 2001, **20**, 1129; (*b*) P. M. Van der Werff, S. R. Batten, P. Jensen, B. Moubaraki and K. S. Murray, *Inorg. Chem.*, 2001, **40**, 1718.
4 S. R. Batten, P. Jensen, B. Moubaraki and K. S. Murray, *Chem. Commun.*, 2000, 2331.
5 (*a*) J. S. Miller, J. C. Calabrese, H. Rommelmann, S. R. Chittipeddi, J. H. Zhang, W. M. Reiff and A. J. Epstein, *J. Am. Chem. Soc.*, 1987, **109**, 769; (*b*) M. L. Talafierro, T. D. Selby and J. S. Miller, *Chem. Mater.*, 2003, **15**, 3602.
6 (*a*) E. Coronado, J. R. Galán-Mascarós, C. Giménez-Saiz, C. J. Gómez-Garcia, J. M. Martínez-Agudo and E. Martínez-Ferrero, *Polyhedron*, 2003, **22**, 2381; (*b*) E. Coronado, A. Forment-Aliaga, J. R. Galán-Mascarós, C. Giménez-Saiz, C. J. Gómez-Garcia, E. Martínez-Ferrero, A. Nuez and F. M. Romero, *Solid State Sci.*, 2003, **5**, 917.
7 (*a*) E. Coronado, J. R. Galán-Mascarós, C. J. Gómez-Garcia and P. Gütlich, *Chem. Eur. J.*, 2000, **6**, 552; (*b*) E. Coronado, J. R. Galán-Mascarós, C. J. Gómez-García, J. M. Martínez-Agudo, E. Martínez-Ferrero, J. C. Waerenborgh and M. Almeida, *J. Solid State Chem.*, 2001, **159**, 391.
8 T. Lancaster, S. J. Blundell, F. L. Pratt, E. Coronado and J. R. Galán-Mascarós, *J. Mater. Chem.*, 2004, **14**, 1518.
9 D. Belo, H. Alves, S. Rabaca, L. C. Pereira, M. T. Duarte, V. Gama, R. T. Henriques, M. Almeida, E. Ribera, C. Rovira and J. Veciana, *Eur. J. Inorg. Chem.*, 2001, 3127.
10 S. Juraja, T. Vu, P. J. S. Richardt, A. M. Bond, T. J. Cardwell, J. D. Cashion, G. D. Fallon, G. Lazarev, B. Moubaraki, K. S. Murray and A. G. Wedd, *Inorg. Chem.*, 2002, **41**, 1072.
11 E. Coronado and C. J. Gómez-García, *Chem. Rev.*, 1998, **98**, 273–296.
12 N. Connelly, *Chem. Rev.*, 1996, **96**, 877.
13 (*a*) R. Hooft, *COLLECT Software*, Nonius BV, Delft, The Netherlands, 1998; (*b*) Z. Otwinowsci and W. Minor, in *Methods in Enzymology*, ed. C. W. Carter and R. M. Sweet, Academic Press, New York, 1996.
14 *XPREP, version 5. 03*, Siemens Analytical X-ray Instruments Inc., Madison, WI, USA, 1994.
15 (*a*) G. M. Sheldrick, *Acta Crystallogr., Sect. A*, 1990, **46**, 467; (*b*) G. M. Sheldrick, *SHELX-97, Program for crystal structure refinement*, University of Göttingen, Germany, 1997 .
16 G. M. Sheldrick, *SHELX-97 Manual*, University of Göttingen, Germany, 1997.
17 (*a*) M.-L. Tong, J. Ru, Y.-M. Wu, X.-M. Chen, H.-C. Chang, K. Mochizuki and S. Kitagawa, *New J. Chem.*, 2003, **27**, 779; (*b*) J. A. Schleuter, J. L. Manson, K. A. Heyzer and U. Geiser, *Inorg. Chem.*, 2004, **43**, 4100.
18 P. M. Van der Werff, S. R. Batten, J. Bevitt, P. Jensen, C. J. Kepert, B. Moubaraki and K. S. Murray, unpublished results.
19 P. Jensen, S. R. Batten, G. D. Fallon, B. Moubaraki, K. S. Murray and D. J. Price, *Chem. Commun.*, 1999, 177.
20 P. Jensen, S. R. Batten, B. Moubaraki and K. S. Murray, *J. Solid State Chem.*, 2001, **159**, 352.
21 P. Jensen, S. R. Batten, B. Moubaraki and K. S. Murray, *Dalton Trans.*, 2002, 3712.
22 G. S. Rushbrooke and P. J. Wood, *Mol. Phys.*, 1958, **1**, 257.
23 R. González, R. Chiozzone, C. Kremer, F. Guerra, G. de Munno, F. Lloret, M. Julve and J. Faus, *Inorg. Chem.*, 2004, **43**, 3013.
24 C. Mathonière, J. Nuttall, S. G. Carling and P. Day, *Inorg. Chem.*, 1996, **35**, 1201.
25 H. Tamaki, Z. Zhong, N. Matsumoto, S. Kida, M. Koikawa, N. Achiwa, Y. Hashimoto and H. Okawa, *J. Am. Chem. Soc.*, 1992, **114**, 6974.
26 D. Armentano, G. De Munno, T. F. Mastropietro, D. M. Proserpio, M. Julve and F. Lloret, *Inorg. Chem.*, 2004, **43**, 5177.